Werk

Terms and Conditions

Contact

Zeitschrift für Geophysik, 1970, Band 36, Seite 531—548. Physica-Verlag, Würzburg

On the Determination of Velocity Depth Distributions of Elastic Waves from the Dynamic Characteristics of the Reflected Wave Field[1])

Von K. FUCHS, Karlsruhe[2])

Eingegangen am 2. April 1970

Summary: Complete synthetic seismograms of *P*-waves reflected from recently proposed crustal and upper mantle models are presented and discussed. It is shown that the fine structure of the models considerably influences the dynamic charateristics of the reflected wave field. Phases expected on the basis of their kinematic characteristics may lack energy and therefore may not be recognized on recorded seismograms. Phases which were believed to be negligible may appear with considerable amplitudes. In some cases the dispersion of seismic waves is so strong as to prevent a travel time analysis. The distribution of the *S*-wave velocity may severely influence the dynamic characteristics of the reflected *P*-waves.

A new iterative scheme is proposed for the inversion of seismic observations into models of the earth's interior. The models are referred to the original observations with the aid of synthetic seismograms. It is recommended that models derived from travel time analysis alone should be verified and improved using synthetic seismograms before conclusions are drawn from the fine structure of seismic models on the mineralogic and geologic properties of crust and upper mantle.

Zusammenfassung: Es werden vollständige synthetische Seismogramme von *P*-Wellen vorgestellt und diskutiert, die aus jüngst vorgeschlagenen Modellen der Kruste und des oberen Mantels zurückgestrahlt werden. Dabei wird gezeigt, daß die Feinstruktur der Modelle die dynamischen Eigenschaften des reflektierten Wellenfeldes merklich beeinflußt. Phasen, die auf Grund ihrer kinematischen Eigenschaften erwartet werden, können so wenig Energie besitzen, daß sie nicht zu beobachten sind. Phasen, die für vernachlässigbar gehalten wurden, können dagegen mit starken Amplituden auftreten. In einigen Fällen ist die Dispersion der seismischen Wellen so stark, daß eine Laufzeitanalyse unmöglich wird. Die Verteilung der *S*-Wellen-Geschwindigkeit kann die dynamischen Eigenschaften der reflektierten *P*-Wellen erheblich beeinflussen.

Ein neues, iteratives Schema zur Inversion seismischer Beobachtungen in Modelle des Erdinnern wird vorgeschlagen. Die Modelle werden über die synthetischen Seismogramme mit den Original-Beobachtungen, den beobachteten Seismogrammen, in Beziehung gesetzt. Es wird empfohlen, Modelle, die nur aus Laufzeituntersuchungen abgeleitet worden sind, mit Hilfe synthetischer Seismogramme zu überprüfen und zu verbessern, bevor aus der Feinstruktur seismischer Modelle Schlüsse auf mineralogische und geologische Eigenschaften der Kruste und des oberen Mantels gezogen werden.

---

[1]) Contribution No. 142 within a joint research program of the Geophysical Institutes in Germany sponsored by the Deutsche Forschungsgemeinschaft (German Research Association).

Contribution No. 50, Geophysical Institute, University Karlsruhe.

[2]) Priv.-Doz. Dr. KARL FUCHS, Geophysikalisches Institut, Universität Karlsruhe, 75 Karlsruhe, Hertzstr. 16, Germany.

1. Introduction

The investigation of crust and upper mantle structure by explosion seismology has progressed considerably during the past decade. The analysis of travel time data from seismic explosion experiments has revealed the gross structure of the crust in most parts of the world. Furthermore, the discussion of the fine structure has become feasible by the improvement of observation and interpretation techniques. Many recent publications in the field of explosion seismology are concerned with the fine structure of the crust and upper mantle.

Zones of reduced velocities have been claimed in the upper and lower crust [LANDISMAN and MÜLLER 1966; MÜLLER and LANDISMAN 1966; FUCHS and LANDISMAN 1966; GIESE 1966, 1968; MEISSNER 1966, 1967]; first order discontinuities have been replaced by transition zones with a continuous depth-velocity distribution [GIESE 1966], a laminated structure has been proposed for the crust-mantle transition [MEISSNER 1967; FUCHS 1969a] and for the low-velocity channel within the upper mantle [AKI 1968].

All models with a fine structure of the crust and upper mantle, different as they are, have one thing in common: they violate the very assumptions on which their derivation has been based.

For a travel time analysis, the a priori assumption tacitly is put into the model that body waves passing through the model are not dispersed or only to a negligible degree. Most crustal models have been derived by the inversion of T, Δ-data. Therefore, it is legitimate to ask whether the dispersion of body waves in presently deduced crustal models is small enough that travel times may be measured with sufficient accuracy.

The construction of seismic models based only on the analysis of travel times of body waves is suffering another drawback, even if dispersion is sufficiently small. T, Δ-data are obtained from observed seismograms by a process termed correlation. The experienced seismologist is trying to identify the class of the model by a comparison of previously computed travel times with the observed travel times of certain phases in the seismic records. In this process, little attention has been paid to the amplitudes of the various phases. Since no reliable amplitude estimates are available during the process of correlation, the seismologist is inclined to pick phases which arrive at the times predicted from the model in his mind, although these phases may lack detectable energy.

In this paper, we will examine to what extent seismic body waves are affected by dispersion when travelling in models recently proposed for the crust and upper mantle in various parts of the world. For these models, synthetic seismogram sections will be computed by the method described by FUCHS [1968a, b]. It will be shown that in some cases the dynamic parameters can be used to distinguish between models which cannot be discriminated on the basis of kinematic parameters alone. Furthermore, we shall demonstrate that there is a number of models which are indistinguishable by their kinematic and dynamic parameters and also by the complete synthetic seismogram section.

2. Propagation of body waves in crustal models

In this part, crustal models are studied which are typical for the fine structures recently derived from detailed travel time analysis of seismic explosion data.

2.1 Sharp or smooth transition?

From the time evidence for an internal layering of the earth's interior was provided by seismology, the question if there is a sharp or smooth transition between these layers has been debated. In most cases, due to the scatter of data the observed travel times have been compatible with both kinds of transition. The final form adopted for the transition was more dependent on the inversion scheme than on the observations. Applying the classical Wiechert-Herglotz method, first-order discontinuities have been excluded from the possible models a priori. In other cases, preference has been given to first-order discontinuities since this facilitates the mathematical treatment of the model considerably. Modern high precision measurements of travel times by controlled explosion experiments have reduced the scatter of the data. In spite of improved accuracy, the range of models compatible with the travel time data is still considerable.

For a long time, it has been felt that the high accuracy of travel times obtained in explosion seismology reduces the variability of crust and upper mantle models significantly to such a degree that false a priori assumptions put into the model would have been detected. There was some truth in this assumption as long as the main goal of crustal investigation was only the mapping of the depth of the main crustal layers. The considerable improvement of seismic crustal data from explosion experiments initiated the interest in the fine structure of the crust and upper mantle. Now the inherent lack of uniqueness of models derived from travel time data alone was realized. There was some hope that dynamic parameters could offer closer bounds on crust and upper mantle models.

In this section we will compare two crustal models (Fig. 1). The travel times of the main phases computed from geometrical ray theory differ by less than 70 msec in the overcritical range which is about the accuracy achieved in crustal investigations, especially for secondary phases. For all practical purposes, these two models cannot be distinguished on the basis of the kinematic parameters of their reflected wave fields.

The model shown in the top part of Fig. 1 represents a discontinuous velocity increase (D). The P-velocity jumps from 6.4 to 7.8 km/sec at the base of a homogeneous layer. This is follwed by a linear increase to 8.6 km/s within a transition layer of 5 km thickness which merges into the homogeneous lower half space at a depth of 35 km (M). A similar model has been discussed by Fuchs [1968c, 1969]. The most remarkable feature of the record section is the phase $\tilde{d}$. It represents a system of multiple reflections being continuously refracted out of the transition zone and interfering constructively with each other. The other phases d (reflection from the discontinuity), d-m (refraction out of the transition zone), and m' (head wave out of the lower half space) are well known from ray geometry.

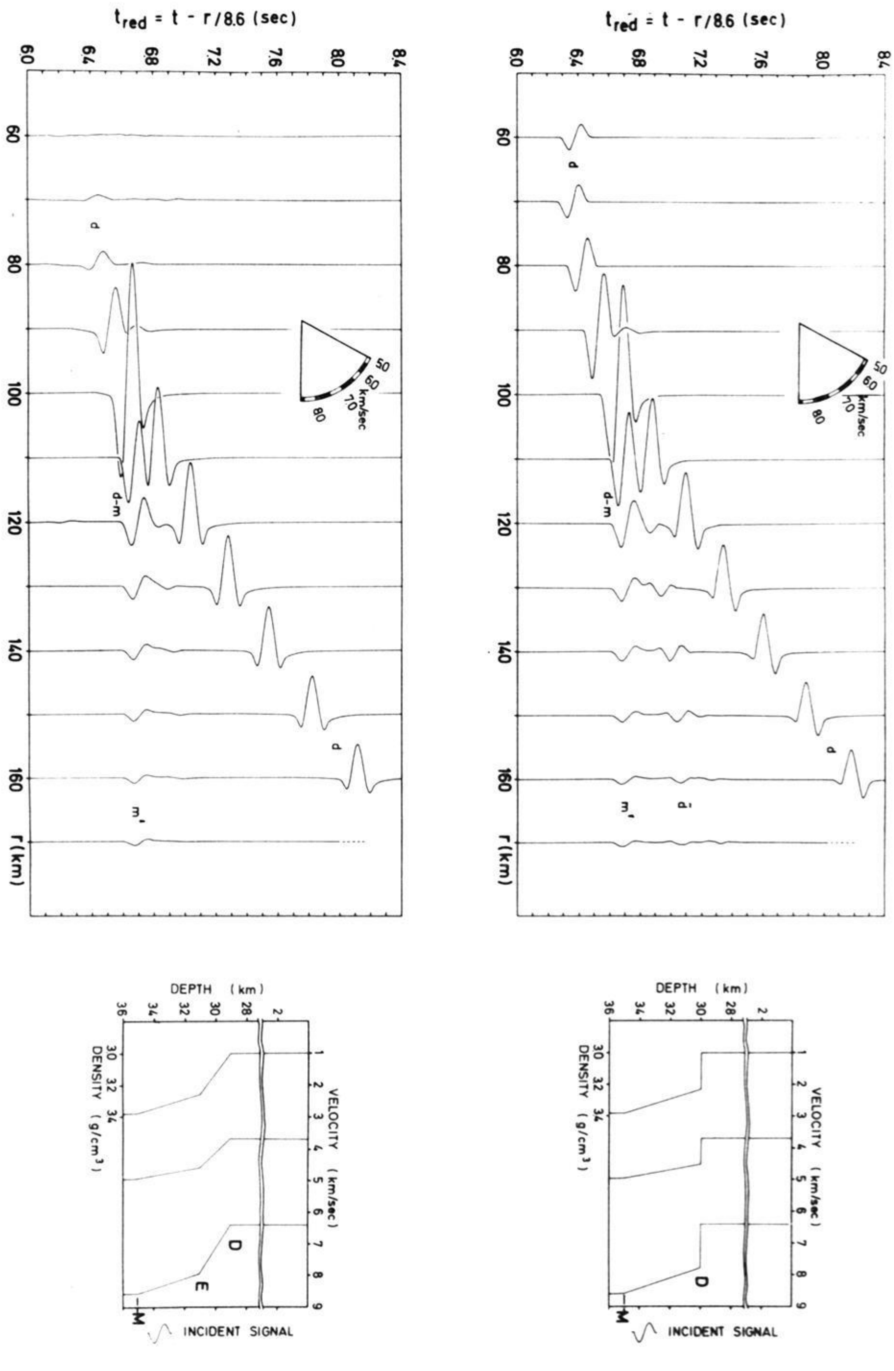
t_red = t - r/8.6 (sec)
6.0
6.4
6.8
7.2
7.6
8.0
8.4
60
80
100
120
140
160
r(km)
d
d-m
m'
50
60
70
80
km/sec
DEPTH (km)
VELOCITY (km/sec)
DENSITY (g/cm3)
D
E
M
INCIDENT SIGNAL

In a number of numerical experiments, the first order discontinuity was replaced by a linear transition zone in such a manner that the travel times remained essentially the same. One example is given in the bottom part of Fig. 1. Here the first-order discontinuity is replaced by a zone in which the *P*-velocity increases linearly from 6.4 to 7.96 km/s between a depth of 29 and 31 km followed by a linear increase to 8.6 km/s to a depth of 35 km.

The phase $\tilde{d}$ has practically disappeared completely. The replacement of the first-order discontinuity by the 2 km-transition zone *DE* has effectively reduced the reflectivity for the internal reflections within the transition zone *EM*. The multiple reflections rapidly loose energy into the upper medium. In all numerical experiments, the phase $\tilde{d}$ was only visible if the thickness of the transition zone was less than 2 km. Therefore, one may use the presence of these secondary arrivals as a measure for the sharpness of a transition zone.

The example discussed above has shown a possible discrimination of two crustal models on the basis of their dynamic parameters taken from synthetic seismograms. We are encouraged to use the dynamic parameters of observed seismograms as an additional source of information on details of crustal structure.

2.2 The *X*-experiment

In this section three crustal models are discussed which differ significantly in the properties of the intermediate layer. The three models are shown in Fig. 2. The zone *DM* is an intermediate layer where velocities and density either increase linearly (top part) or are constant (middle part) or decrease linearly (bottom part) in such a manner that the vertical travel time through the three models remains the same. The distributions of velocities and density in the inhomogeneous intermediate layer in the top and bottom part of Fig. 2 form the two legs of the capital *X*. Therefore, the term "*X*-experiment" has been chosen.

The model with a positive gradient (Fig. 2, top) has already been discussed in the preceding section 2.1. The small discontinuity at *M* does not influence the computed seismograms significantly. We observe again the reflection *d* from the top *D* of the transition zone, the phase *d-m* continuously refracted out of *DM*, the headwave m' from the lower half space and the phase $\tilde{d}$ discussed in the previous section.

Fig. 1: Comparison of two transition zones with equal vertical transit time.

Top: Linear transition zone of 5 km thickness below a first-order discontinuity. The reverberations $\tilde{d}$ following the head wave m' from the lower half space form a system of multiple reflections being continuously refracted out of the transition zone and interfering constructively with each other.

Bottom: The first-order discontinuity has been replaced by an additional linear transition zone between *D* and *E*. Note the disappearance of the reverberations $\tilde{d}$.

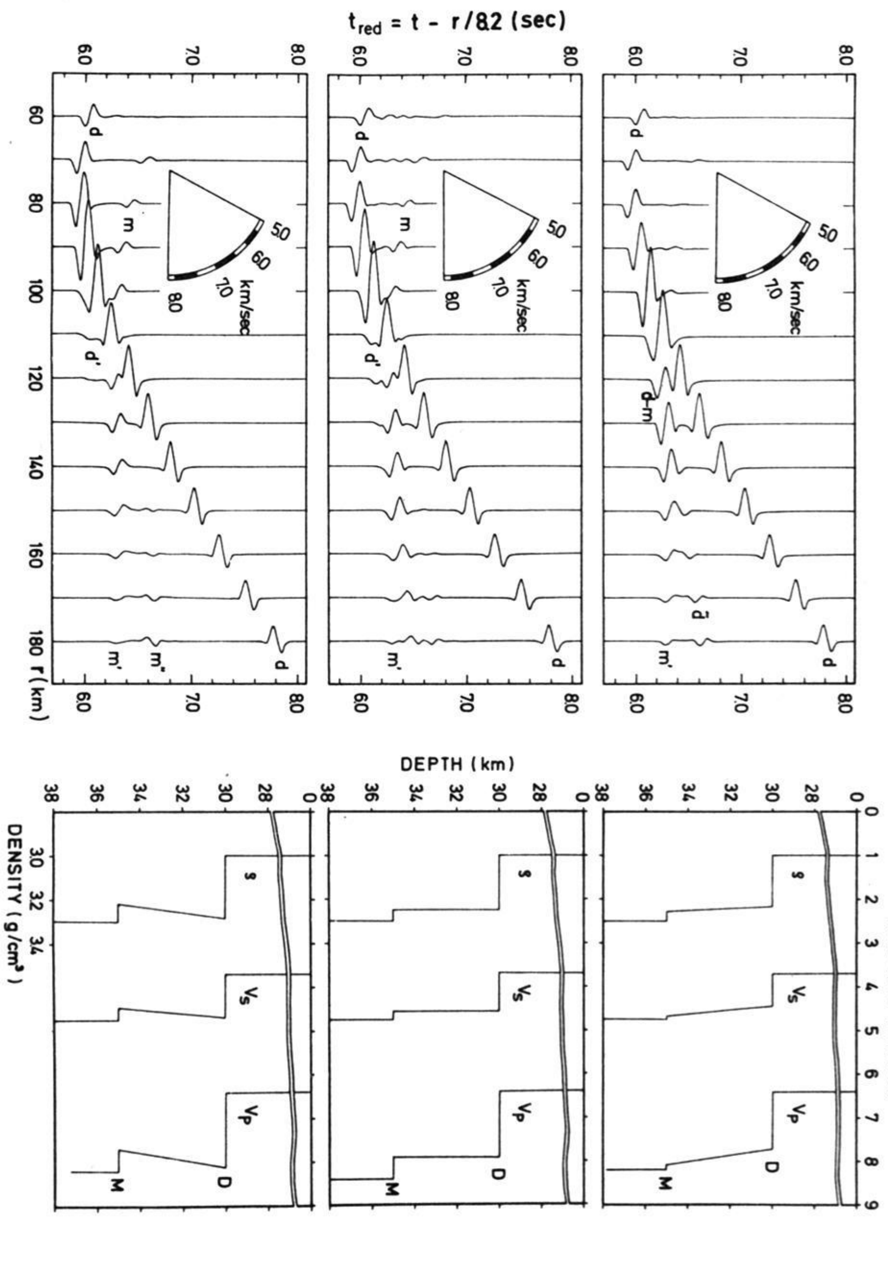
t_red = t - r/8.2 (sec)
r (km)
km/sec
DEPTH (km)
VELOCITY (km/sec)
DENSITY (g/cm³)

In the case of a homogeneous intermediate layer (Fig. 2, middle) the main phases d and m' essentially remain the same as in the top part. The phase d' is the headwave from the top of the homogeneous layer. It replaces the phase *d-m*. The headwave m' is followed again by reverberating signals. These are formed by the interference of phase d', the reflection m and the reflection of type *PP* between bottom and top of the intermediate layer. This reflection generates another headwave m'' out of the lower half space.

The negative gradient layer (Fig. 2 bottom) forms a kind of low-velocity channel with a smooth upper boundary. The main phases d and m' are the same as in the previous cases. Although no headwave is expected out of the transition zone with a negative velocity gradient, the phase d' can clearly be recognized to a distance of about 120 km. This is a truly diffracted wave not predicted by ray optics.—The phase m'' travels with the same velocity as m'. It is the second headwave guided at the *M*-discontinuity with the *P*-velocity of the lower half space. It is generated by a *PP*-reflection between top and bottom of the negative gradient layer.

Comparing all three record sections corresponding to the different crustal models in Fig. 2, it must be emphasized that not only the main phases like m' and d appear to be indistinguishable but also phases with minor amplitudes like d' and *d-m*. Only a very careful analysis of the velocities of the phases m'' and $\tilde{d}$ could discriminate the two crustal models with the positive and negative gradient. However, it seems unlikely that such a distinction can be made on records observed in the field since the signal/noise ratio is several orders of magnitude larger than on synthetic seismograms. In fact, by adding some uncorrelated or signal generated noise the phases on the three record sections would become indistinguishable.

In conclusion it is practically not possible to discriminate the three crustal models from the seismograms observed at overcritical distances.

2.3 Low-velocity channel

The existence of low-velocity channels in the upper and lower crust as well as in the upper mantle has been proposed by several authors. It is the purpose of this section to study the dynamic properties of waves reflected by crustal structures which comprise a low-velocity channel. The four crustal models to be discussed are presented in Fig. 3 and denoted by I-IV. All four models incorporate a low-velocity channel *EM* and its lid *DE*.

Fig. 2: The *X*-experiment. Three different types of transition layers *DM* produce quite similar reflected wave patterns. Top: linearly increasing velocities; middle: homogeneous layer; bottom: linearly decreasing velocities.

Fig. 3: The effect of a low-velocity channel.
I: High-speed lid (V_p = 7.9 km/s). II: Velocities in the upper half space and the lid have been reduced. III: Compared to II only V_s in the channel has been reduced. IV: Compared to II the homogeneous channel is replaced by a laminated zone.

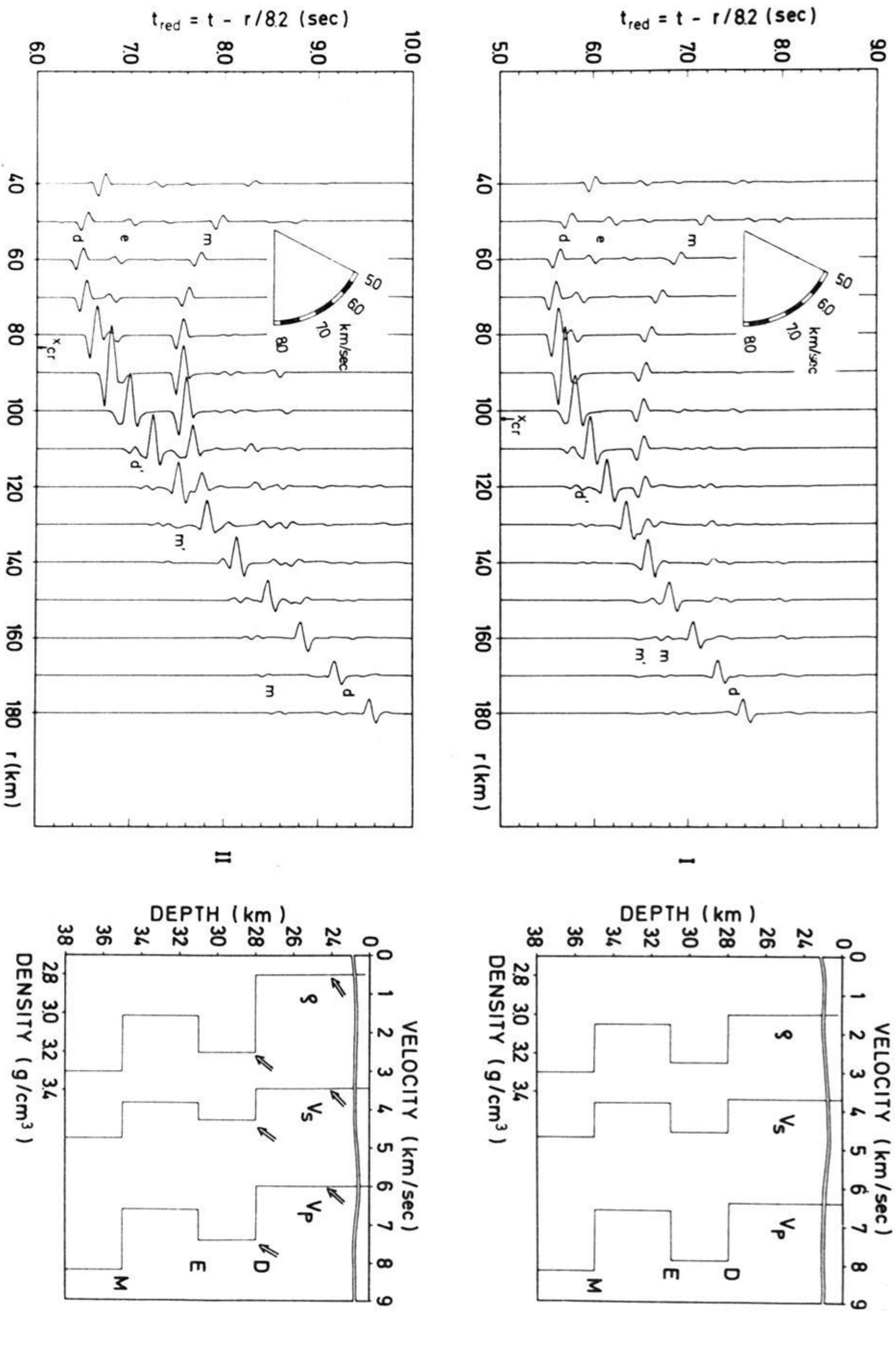

$t_{red} = t - r/8.2$ (sec)
r (km)
km/sec
I
II
VELOCITY (km/sec)
DEPTH (km)
DENSITY (g/cm^3)
V_S
V_P
D
E
M

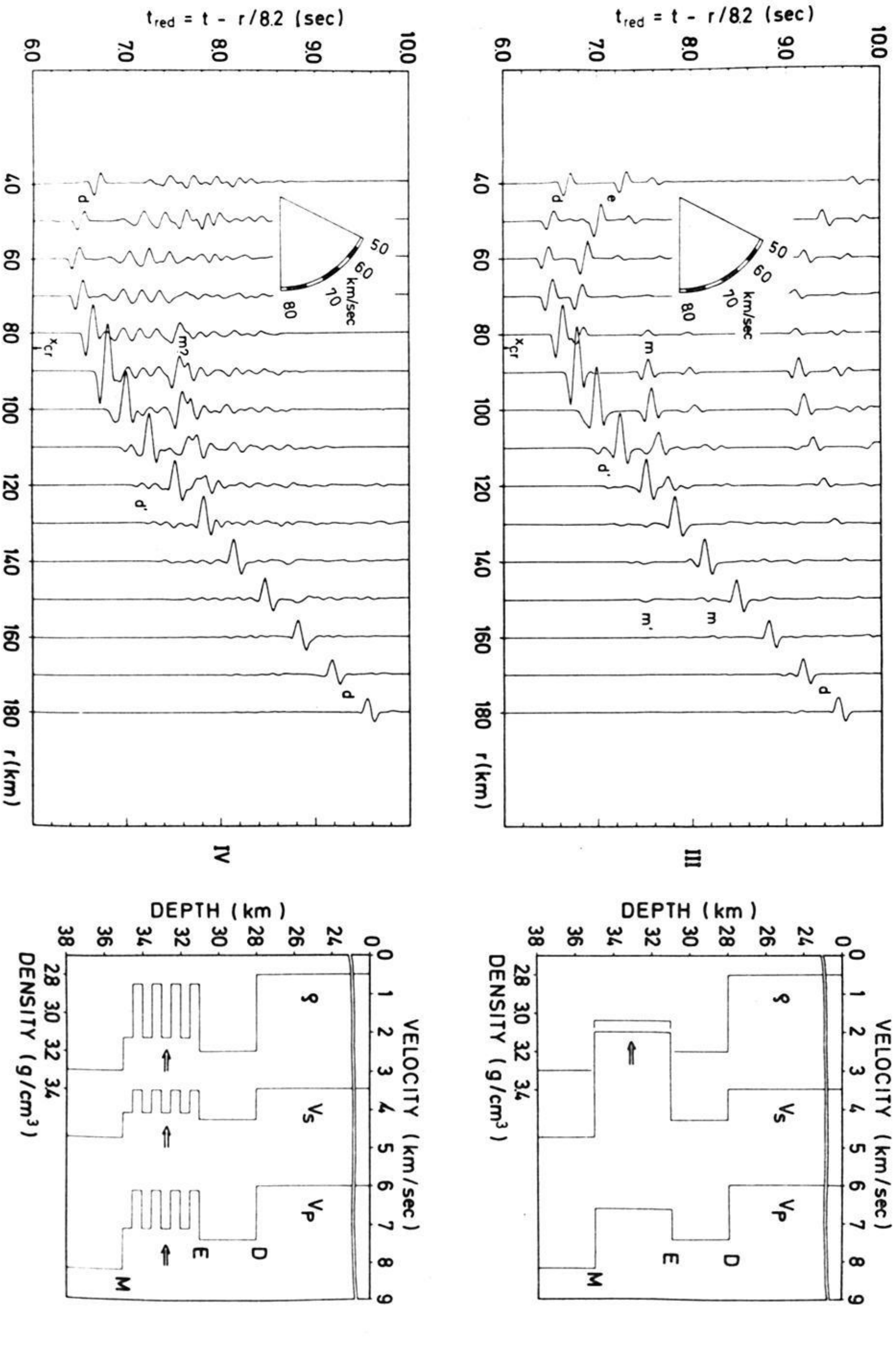
t_red = t - r/8.2 (sec)
r (km)
km/sec
III
IV
DEPTH (km)
VELOCITY (km/sec)
DENSITY (g/cm³)
ρ
Vs
Vp
D
E
M

The main phases of the reflected wave field in **case I** are as follows: d is the reflection from the top D of the lid. The reversed sign of the reflection e from the bottom of the lid is caused by the negative sign of the reflection coefficient at E. The headwave d' from the lid of the channel begins to interfere with the reflection e at about 120 km. Beyond 140 km destructive interference prevents further observation of both phases.

The most striking feature of the reflection m from the bottom of the channel is the absence of an amplitude maximum in the vicinity of the critical distance at x_{cr} = 103,0 km. Furthermore, a very rapid decay of the m amplitudes must be noted at distances larger than about 130 km. The phase m can hardly be detected beyond 160 km. The amplitudes of the headwave m' from the lower halfspace are weaker as well.

In the absence of a low-velocity zone the reflection m usually forms a dominant phase and is often used to derive the velocity distribution at the crust-mantle boundary. If no attention is paid to the possibly weak amplitudes a false correlation with noise or other phases is very likely.

The low amplitudes must be attributed partly to strong geometrical spreading of the ray bundle caused by the rather high velocity in the lid of the channel. In the crustal **model II** the velocities and density of the upper halfspace and the lid of the channel have been reduced. The headwave d' travels with a velocity of 7.4 km/sec. Destructive interference with the reflection e causes the disappearance of the two phases at distances beyond 140 km.—The reflection m reaches an amplitude maximum which is slightly displaced to distances larger than critical. Beyond 130 km again a rapid decay of amplitudes renders the phase m to be not detectable on observed seismograms.

So far v_S was assumed to be $v_P/\sqrt{3}$, corresponding to a Poisson ratio of 0.25. Since we are concerned with the reflected P-field usually the choice of the S-velocities is not regarded as critical. In crustal **model III** only the velocity of the S-wave in the low velocity channel has been reduced to 2.0 km/sec. Such a reduction is caused by an increase in temperature. All other parameters remain as in **model II**. The record section contains some unexpected features:

- the amplitudes of the reflection m at distances smaller than critical have decreased strongly
- the reflection e from the bottom of the lid has considerably increased its amplitude and
- the reflection e has reversed its polarity which is now the same as that of the reflection d from the top of the lid
- the comparatively strong phases at a reduced time of about 9 sec are caused by P-waves which have traversed the channel twice as converted S-waves and returned to the surface as P-waves

The discussion of crustal **model III** demonstrates very clearly that the reflected P-waves may be considerably influenced by the S-wave velocities.

It has also been suggested that the low-velocity channels may contain a number of laminas with increased velocity as shown in **model IV**. What is the appearance of P-waves reflected from such a laminated channel? The most prominent feature are the strong reverberations following the reflections e and m. The reflection m is nearly completely masked by the reverberations.

2.4 The laminated transition zone

A laminated transition zone between crust and upper mantle has been proposed as explanation for anisotropy [Meissner 1967]. Also strong near vertical reflections of high frequency could be explained by such a structure of the crust-mantle boundary [Fuchs 1968a]. In this section it will be examined how a laminated transition zone will influence the reflected wave field.

In Fig. 4 two crustal models with equal vertical transit time are compared. In the lower part of the figure the zone DM is formed by a transition layer in which V_p rises linearly from 7.8 to 8.6 km/sec. At D the velocity increases discontinuously from 6.4 to 7.8 km/sec.

The laminated transition zone in the top part of Fig. 4 consists of 10 high velocity layers ($V_p = 8.6$ km/sec) and 10 low velocity layers ($V_p = 7.8$ km/sec) of thickness 250 m in alternating order.

The record section of the linear transition zone displays the same features as that of Fig. 1 (top part). It has already been discussed in detail. The clear onset of the headwave m' from the lower halfspace should be noted for comparison with the top part of Fig. 4. It coincides very closely with the theoretical arrival time marked by small dashes. The other phases d, d-m and $\tilde{d}$ have the same origin as discussed in Fig. 1.

Turning to the record section of the laminated transition zone it is most surprising that practically no energy arrives as headwave from the lower halfspace. Instead, a strong phase is observed with no definite beginning. Its group velocity is estimated to about 8.2—8.3 km/sec. This wave train is strongly dispersed. Its dispersion is not caused by the finite thickness of the laminas. Decreasing their thickness to 125 m and doubling their number do not change essentially the record section. The dispersion is caused by the whole laminated transition zone DM of thickness 5 km. This zone can be regarded as a transversely anisotropic plate between two isotropic halfspaces. The dispersed wave train is a kind of plate wave. An analysis in terms of travel times does not seem to be appropriate for this kind of wave propagation which may be regarded as a leaking mode.

According to Brekhovskikh [1960] the velocity parallel and vertical to the lamination of an infinitely periodic structure is $V_= = 8.2$ and $V_\perp = 8.15$ km/sec, respectively. The factor of anisotropy is $A = 2(V_= - V_\perp)/(V_= + V_\perp) = 0.6\%$, only. This is a very modest amount of anisotropy compared to 10% or 20% which has been proposed for the upper mantle. Even such a small amount as 0.6% very strongly affects the record section. The phase d reflected from the top D of the laminated plate is practically not influenced by the transition zone showing only very weak reverberations.

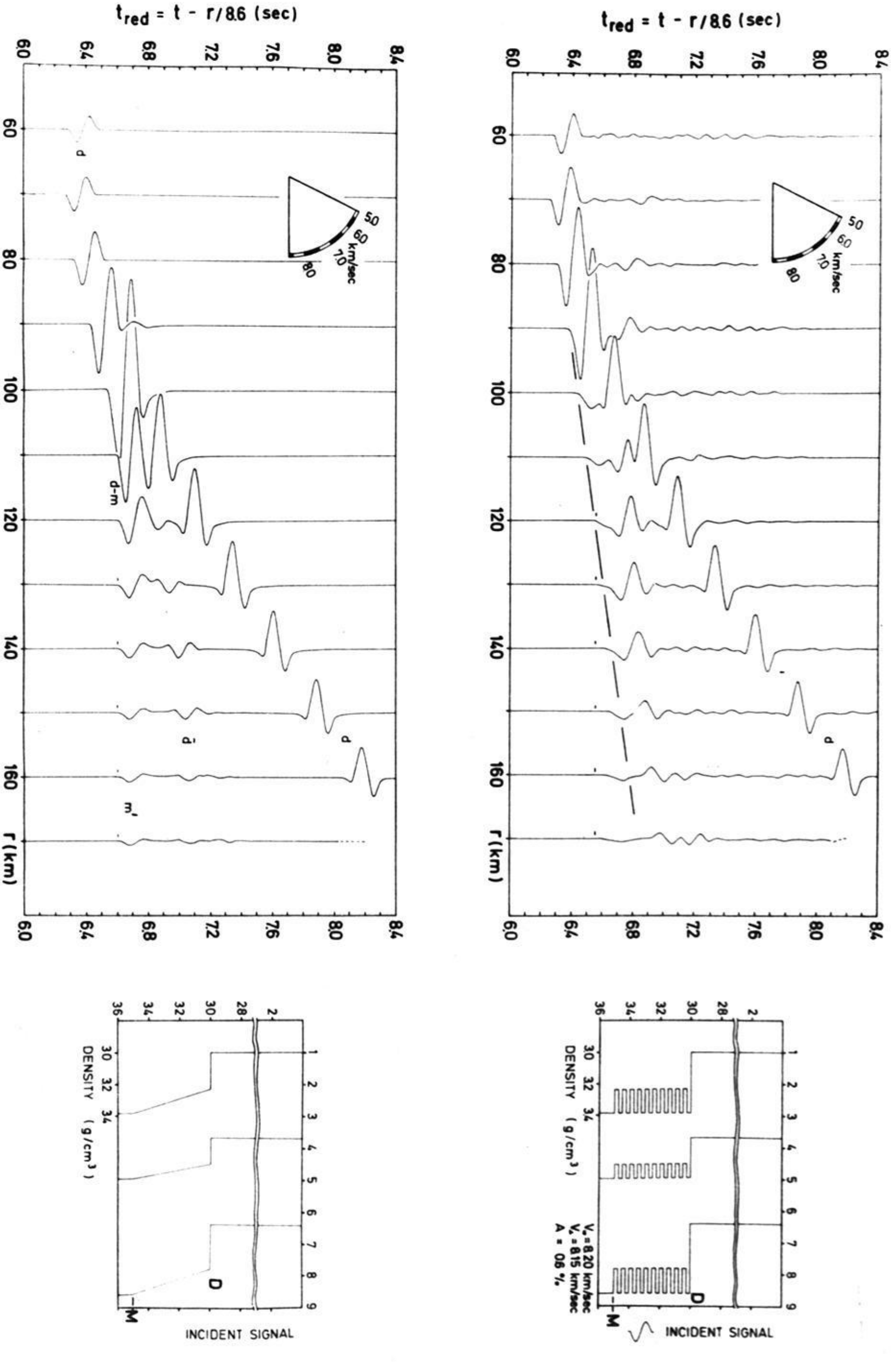

t_red = t - r/8.6 (sec)
r (km)
km/sec
DENSITY (g/cm³)
INCIDENT SIGNAL
D
M

In Fig. 5 the factor of anisotropy is increased to 6.6% (top part) and 21.9% (bottom part). The duration of the response of the transition zone is increased considerably in both cases by strong reverberations.

In the top part of the figure we find some indications for a phase m reflected from the bottom M of the laminated zone. It merges into the dispersed plate wave described earlier.—In the bottom part of Fig. 5 the strong anisotropy has been achieved by a strong decrease of V_S in the low-velocity lamellas. Partial melting in these laminas could be responsible. Now the response time of the transition zone is longer than 5 sec. The only phase which can be identified with certainty is the reflection d from the top of the transition zone. The other phases should be better analyzed in terms of leaking modes than in terms of travel times of body waves. For comparison the travel time curve for a hypothetical phase m'—head wave from the laminated crust-mantle transition—with a velocity $V_= = 7.27$ km/sec is indicated by the dashed line. No arrival of energy can be detected along this line.

The numerical experiments on wave propagation in laminated media are far from complete. However, they have indicated already that even in the case of modest anisotropy of 0.6% an analysis in terms of travel times is questionable. For the stronger anisotropy cited in the literature it seems highly unlikely that it could have been detected by a travel time analysis.

3. Construction of seismic models

The original seismic observations are the seismograms at various distances from the source. These observations must be inverted into models of the earth's interior. The inversion technique commonly used is demonstrated in the top part of Fig. 6. The most important step during this inversion is a process termed correlation by which corresponding seismic phases are identified and their travel times determined. These travel times $T(\Delta)$ and/or their derivatives $dT/d\Delta$ as a function of distance are often taken as the original observations. There are several methods of inverting these 'observed' parameters into the parameters of the model, e.g. distribution of P and S-velocities and density.

In most methods the final model is not derived directly. Instead, a working model as a first estimate is improved by the iteration indicated in the figure: the theoretical

Fig. 4: Comparison of linear with laminated transition zone of equal vertical transit time.

Top: Laminated transition zone of high ($V_P = 8.6$ km/s) and low velocity ($V_P = 7.8$ km/s). Thickness of single lamina 250 m. This medium corresponds to a transversely isotropic layer with a factor of anisotropy of 0.6%.

Bottom: Linear transition zone below first-order discontinuity (see Figure 1, top).

Fig. 5: Effect of anisotropic transition layers. The laminated transition zone corresponds to a transversely isotropic layer. Top: Factor of anisotropy 6.6%. Bottom: 21.9% anisotropy.

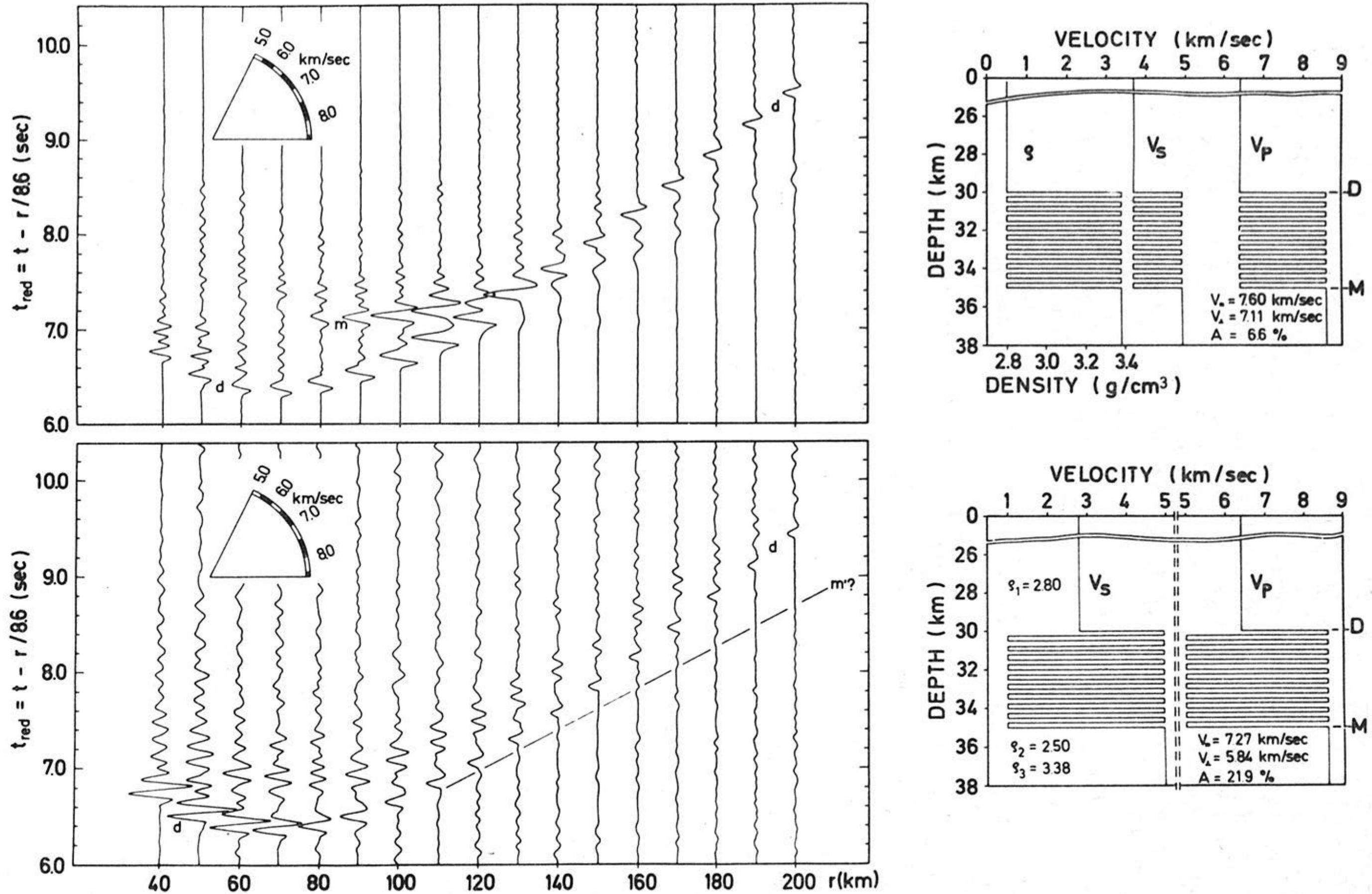

t_{red} = t - r / 8.6 (sec)
10.0
9.0
8.0
7.0
6.0
50
60
70
80
km/sec
d
m
m'?
40
60
80
100
120
140
160
180
200
r(km)
VELOCITY (km/sec)
DEPTH (km)
DENSITY (g/cm³)
2.8 3.0 3.2 3.4
ϱ
V_S
V_P
D
M
V_o = 7.60 km/sec
V_Δ = 7.11 km/sec
A = 6.6 %
ϱ_1 = 2.80
ϱ_2 = 2.50
ϱ_3 = 3.38
V_o = 7.27 km/sec
V_Δ = 5.84 km/sec
A = 21.9 %

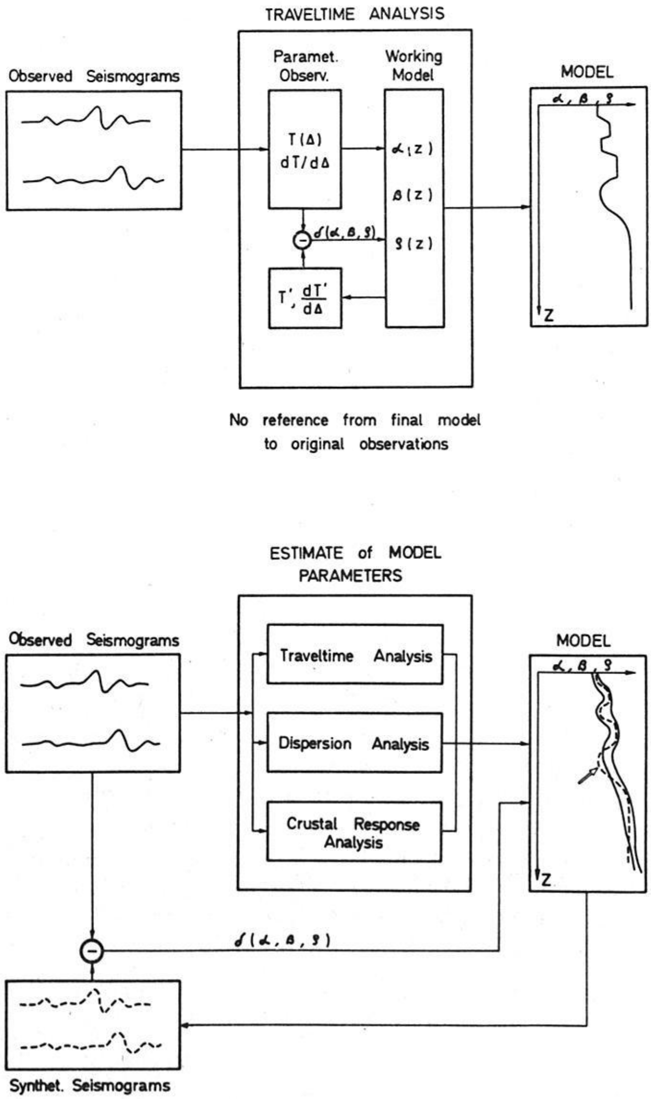

Fig. 6: The construction of seismic models from observed seismograms.

Top: The original observations are never referred to, once the correlation of seismic phases is completed.

Bottom: Synthetic seismograms as a link between original observations and seismic model.

parameters T' and/or $dT'/d\Delta$, computed for the working model, are compared with the 'observed' parameters. The residuals are used to correct the working model until they become small enough. As soon as the 'observed' parameters sufficiently match the computed ones, the working model is considered as the final model compatible with the so-called observations.

It should be noted, however, that the original observations—the seismograms—are never referred to, once the correlation of seismic phases has been completed. A correlation error may never be detected if a model with sufficiently small residuals is derived.

The study of synthetic seismograms presented in this paper has revealed three major sources of errors during the process of correlation:

— strong reverberations—like phase $\tilde{d}$ in Fig. 1 and 4—may be taken as separate branches of the travel time curve

— a rapid decay of amplitudes along a certain branch—like m in Fig. 3—may lead to a false continuation of the correlation either with noise or irrelevant signals

— for strongly dispersed phases a distinct arrival is hard to identify—e.g. propagation in laminated media Fig. 4 and 5—misreadings in time are very likely.

Within the inversion scheme in the top part of Fig. 5 false correlations may never be detected although the model residuals are vanishing. The iteration process ends in a vicious circle detached from the original observations.

A better guarantee that the final model is compatible with the observed seismograms is obtained by a comparison of observed and synthetic seismograms. It is proposed, therefore, that the inversion of seismic observations into models of the earth's interior proceeds as indicated in the lower part of Fig. 6. The travel time analysis of the observed seismograms is used to estimate the parameters of the crustal model (dashed line). This estimate should be supplemented by dispersion analysis of normal and leaking modes and a crustal response study [BONJER, FUCHS, and WOHLENBERG 1969]. The model corrections δ (α, β, ϱ) are then obtained from a comparison of observed and synthetic seismograms. The final model is established by iteration if the residuals become sufficiently small. There is not only one model compatible with the observed seismograms but rather a range of models. It is indicated in the figure that the first estimate may be partly outside of this range.

4. Conclusions

It was the purpose of this communication to present some examples of complete synthetic seismograms for some recently proposed crustal models. It is shown that the fine structure of these vertically inhomogeneous models considerably affects the dynamic characteristics of the reflected wave field, causing secondary phases not to be explained by ray optics, rapid decay of amplitudes and strong dispersion. The distribution of S-wave velocities may notably influence the dynamic properties of the reflected P-waves. In some cases it may become necessary to replace the analysis in terms of travel times by a dispersion analysis of leaking modes.

The consideration of the dynamic parameters puts sharper limits on crust and upper mantle models than the analysis of the kinematic parameters alone. In view of the present study it is most likely that attempts to determine the fine structure of crustal models from a travel time analysis have been too optimistic in the past. It is recommended that crustal models derived from travel times should be verified and improved with the aid of synthetic seismograms before detailed conclusions are drawn on the mineralogic and geologic properties of the crust and upper mantle. It is quite possible that in the future seismic models may become less accurate but more reliable.

A new iterative scheme for the inversion of seismic observations into model parameters of the earth's interior is proposed where the derived model is directly referred to the original observations by means of synthetic seismograms.

5. Acknowledgements

The author is indepted to Prof. Stephan Müller and Dr. G. Müller for fruitful discussions. Dr. Prodehl critically read the manuscript. This work is sponsored by the Deutsche Forschungsgemeinschaft. Computing facilities were made available partly at the Deutsches Rechenzentrum Darmstadt and partly at the Gesellschaft für Kernforschung Karlsruhe.

References

Aki, K.: Seismological evidences for the existence of soft thin layers in the upper mantle under Japan. J. Geophys. Res. 73 (2), 585—594, 1968

Brekhovskikh, L. M.: Waves in layered media, Transl. by D. Liebermann. Acad. Press, New York, 561 p., 1960

Fuchs, K.: Die Reflexion von Kugelwellen an inhomogenen Übergangszonen mit beliebiger Tiefenverteilung der elastischen Moduln und der Dichte. Habilitationsschrift, Universität Karlsruhe, 136 p., 1968a

—: The reflection of spherical waves from transition zones with arbitrary depth-dependent elastic moduli and density. J. Phys. Earth 16, Spec. Iss., 1968b

—: On the properties of deep crustal reflectors. Z. Geophys. 35, 133—149, 1969a

—: The method of stationary phase as a diagnostic aid in estimating the field pattern of body waves reflected from transition zones. Z. Geophys. 35, 431—435, 1969b

Fuchs, K., and M. Landisman: Detailed crustal investigation along a North-South section through the central part of Western Germany, AGU Monogr. Ser. 10, 433—452, 1966

Giese, P.: Versuch einer Gliederung der Erdkruste im nördlichen Alpenvorland, in den Ostalpen und in Teilen der Westalpen mit Hilfe charakteristischer Refraktionslaufzeitkurven, sowie eine geologische Deutung. Habilitationsschrift, Freie Universität Berlin, 1966

—: The structure of the earth's crust in central Europe. 10th Gener. Ass. Europ. Seism. Comm., Leningrad, 30 p., 1968

Landisman, M., and St. Müller: Seismic studies of the earth's crust in continents, 2. Analysis of wave propagation in continents and adjacent. Geophys. J. 10, 539—548, 1966

Meissner, R.: An interpretation of the wide angle measurements in the Bavarian Molasse basin. Geophys. Prosp. 14 (1), 7—16, 1966

—: Zum Aufbau der Erdkruste. Ergebnisse der Weitwinkelmessungen im bayerischen Molassebecken. Gerl. Beitr. Geophys. 76, 211—254 and 295—314, 1967

Müller, St., and M. Landisman: Seismic studies of the earth's crust in continents; part I: evidence for a low-velocity zone in the upper part of the lithosphere. Geophys. J. 10, 525 to 538, 1966